

Understanding the Molecular Basis for the Inhibition of the Alzheimer's A β -Peptide Oligomerization by Human Serum Albumin Using Saturation Transfer Difference and Off-Resonance Relaxation NMR Spectroscopy

Julijana Milojevic, Veronica Esposito, Rahul Das, and Giuseppe Melacini*

Contribution from the Departments of Chemistry, Biochemistry and Biomedical Sciences, McMaster University, 1280 Main Street West, Hamilton, Ontario, L8S 4M1, Canada

Received October 13, 2006; E-mail: melacini@mcmaster.ca

Abstract: Human serum albumin (HSA) inhibits the formation of amyloid β -peptide (A β) fibrils in human plasma. However, currently it is not known how HSA affects the formation of the highly toxic soluble diffusible oligomers that occur in the initial stages of A β fibrillization. We have therefore investigated by solution NMR the interaction of HSA with the A β (12–28) peptide, which has been previously shown to provide a reliable and stable model for the early prefibrillar oligomers as well as to contain key determinants for the recognition by albumin. For this purpose we propose a novel NMR approach based on the comparative analysis of A β in its inhibited and filtrated states monitored through both saturation transfer difference and recently developed nonselective off-resonance relaxation experiments. This combined NMR strategy reveals a mechanism for the oligomerization inhibitory function of HSA, according to which HSA targets preferentially the soluble oligomers of A β (12–28) rather than its monomeric state. Specifically, HSA caps the exposed hydrophobic patches located at the growing and/or transiently exposed sites of the A β oligomers, thereby blocking the addition of further monomers and the growth of the prefibrillar assemblies. The proposed model has implications not only for the pharmacological treatment of Alzheimer's disease specifically but also for the inhibition of oligomerization in amyloid-related diseases in general. In addition, the proposed NMR approach is expected to be useful for the investigation of the mechanism of action of other oligomerization inhibitors as well as of other amyloidogenic systems.

Introduction

A hallmark of Alzheimer's disease (AD) is the deposition of amyloid plaques in the brain parenchyma and in the meningeo-cerebral blood vessels.^{1–4} The primary component of AD amyloid deposits is the 40–42 amino acid β -peptide (A β) resulting from the proteolytic processing of the ubiquitous transmembrane β -amyloid precursor protein.^{5–7} Most nucleated cells in the body secrete the A β polypeptide, but A β aggregates into amyloid fibrils exclusively in the central nervous system (CNS) and not in peripheral tissues.^{7,8} The absence of A β fibril depositions in such tissues is the result of the presence of A β -carrier plasma proteins that are able to inhibit A β -amyloid

deposition.^{9,10} Essentially the same carrier proteins are present in the cerebrospinal fluid (CSF) as well but at about a 1000-fold lower concentration,¹¹ thus significantly reducing their inhibitory effect on amyloid formation in CSF as compared to plasma. Most of the amyloid-inhibitory activity of plasma is accounted for by human serum albumin (HSA),¹⁰ which is the most abundant protein in both plasma and CSF.^{9,12} The IC₅₀ value (10 μ M) for the inhibition by albumin of A β (1–40) incorporation into existing β -amyloid fibrils is significantly lower than the concentration of HSA in plasma (644 μ M) but higher than the concentration of HSA in the CSF (3 μ M), consistently with amyloid fibrils being found selectively in the CNS but not in peripheral tissues.¹⁰

Despite the physiological relevance of the HSA–A β peptide interaction, the current understanding of the molecular basis for the recognition of A β by HSA is still limited and several key

- (1) Seubert, P.; Vigo-Pelfrey, C.; Esch, F.; Lee, M.; Dovey, H.; Davis, D.; Sinha, S.; Schlossmacher, M.; Whaley, J.; Swindlehurst, C.; McCormack, R.; Wolfert, R.; Selkoe, D.; Lieberburg, I.; Schenk, D. *Nature* **1992**, *359*, 325–327.
- (2) Van Gool, W. A.; Kuiper, M. A.; Walstra, G. J. M.; Wolters, E. C.; Bolhuis, P. A. *Ann. Neurol.* **1995**, *37*, 225–230.
- (3) Motter, R.; Vigo-Pelfrey, C. *Ann. Neurol.* **1995**, *38*, 643–648.
- (4) Scheuner, D. et al. *Nat. Med.* **1996**, *2*, 864–870.
- (5) Tanzi, R. E.; Gusella, J. F.; Watkins, P. C.; Bruns, G. A.; St. George-Hyslop, P.; Van Keuren, M. L.; Patterson, D.; Pagan, S.; Kurnit, D. M.; Neve, R. L. *Science* **1987**, *235*, 880–884.
- (6) Kang, J.; Lemaire, H. G.; Unterbeck, A.; Salbaum, J. M.; Masters, C. L.; Grzeschik, K. H.; Multhaup, G.; Beyreuther, K.; Muller-Hill, B. *Nature* **1987**, *325*, 733–736.
- (7) Haass, C.; Selkoe, D. J. *Cell* **1993**, *75*, 1039–1042.
- (8) Haass, C.; Hung, A. Y.; Schlossmacher, M. G.; Oltersdorf, T.; Teplow, D. B.; Selkoe, D. J. *Ann. N.Y. Acad. Sci.* **1993**, *695*, 109–116.

- (9) Biere, A. L.; Ostaszewski, B.; Stimson, E. R.; Hyman, B. T.; Maggio, J. E.; Selkoe, D. J. *J. Biol. Chem.* **1996**, *271*, 32916–32922.
- (10) Bohrmann, B.; Tjernberg, L.; Kuner, P.; Poli, S.; Levet-Trafit, B.; Naslund, J.; Richards, G.; Huber, W.; Dobeli, H.; Nordstedt, C. *J. Biol. Chem.* **1999**, *274*, 15990–15995.
- (11) Hardman, J. G.; Limbird, L. E.; Molinoff, P. B.; Ruddon, R. W.; Gilman, A. G. *Goodman & Gilman's The Pharmacological Basis of Therapeutics*, 9th ed.; McGraw-Hill: New York, 1996.
- (12) Kuo, Y. M.; Kokjohn, T. A.; Kalback, W.; Luehrs, D.; Galasko, D. R.; Chevallier, N.e.; Koo, E. H.; Emmerling, M. R.; Roher, A. E. *Biochem. Biophys. Res. Commun.* **2000**, *268*, 750–756.

questions about the amyloid-inhibitory mechanism of HSA remain unanswered. For instance, a growing body of evidence points to soluble diffusible oligomers formed in the fibrillation pathways as the main toxic species responsible for AD.^{13,14} However, it is not known how albumin affects the initial steps of A β oligomerization. Hence we have investigated using solution NMR the interaction between HSA and the A β (12–28) peptide, which spans the central hydrophobic core of A β (L₁₇VFFA₂₁),^{15–17} and it has been previously shown to provide a reliable and stable model for the early prefibrillation oligomerization equilibria of A β .¹⁵ Furthermore, this peptide is also suitable to investigate the effect of albumin because key binding sites for HSA are confined to the A β (1–28) segment,¹⁸ but the first 11, mostly hydrophilic, N-terminal residues are not significantly involved in self-recognition.¹⁹

Solution NMR experiments have the ability to probe at residue and atomic resolution not only the monomeric state of A β (12–28)²⁰ but also its self-assembled forms including the soluble oligomers.^{21–24} Specifically, 2D-saturation transfer difference (STD)^{22,23} and recently developed off-resonance relaxation (ORR)²⁴ experiments measure cross- and self-relaxation rates, respectively, which are very sensitive to the presence of soluble high molecular weight (MW) species in fast dynamic exchange with the monomers and are therefore excellent probes for the reversible pre-nuclear self-association equilibria.²⁴ Here, we have employed a combined STD/ORR approach to monitor the effect of both albumin addition and filtration on the peptide under investigation. The comparative analysis of the STD/ORR data for the inhibited and filtered states reveals that HSA not only interacts preferentially with the prefibrillar oligomeric species but also targets and caps the exposed hydrophobic sites within the oligomers, thus preventing further monomer addition and exchange. The resulting model rationalizes the A β oligomerization inhibition function of HSA.

Materials and Methods

Sample Preparation. The Alzheimer's peptide fragment A β (12–28) (¹H₃N–V₁₂HHQKLVFFAEDVGSNK₂₈–COO[–]) with a purity of 98.6% was purchased from Genscript Corp., Piscataway, NJ. 1 mM A β (12–28) samples for NMR analysis were prepared by dissolving a weighed amount of lyophilized peptide in 50 mM deuterated (*d*₄) sodium acetate buffer, pH 4.7 (uncorrected for isotope effects), containing 90% doubly distilled H₂O and 10% D₂O (Cambridge Isotope Laboratories). After the peptide was dissolved in the buffer, solutions were centrifuged for 5 min at 2000 rpm and 4 °C. The stability over

time of the samples prepared according to this protocol was monitored by 1D spectra as shown in Figure S1 (left panels). HSA (Sigma) was 99% pure, fatty acid free, and essentially globulin free. For the titration experiments, aliquots from concentrated stock HSA solutions (0.2 mM, 1.5 mM, and 3 mM HSA) were added to the 1 mM A β (12–28) NMR sample. 1.5 mM and 0.2 mM HSA stock solutions were obtained by dilution of the 3 mM HSA solution. Addition from different stock solutions was performed to minimize volumetric errors (the smallest volume added was 1 μ L) and also to reduce dilution effects. The total volume added was less than 20 μ L, and therefore the dilution effects were negligible (<4%). The NMR spectra were recorded immediately after addition of HSA, and the samples were stable after each HSA addition. This was confirmed by a 1D experiment recorded before and after each titration point.

Filtration Protocol. Ultrafree-MC Millipore 30 kDa cutoff filters were used. Glycerol was removed from the filters by washing with 50 mM deuterated (*d*₄) sodium acetate buffer at least five times. Filtration was performed at room temperature by centrifugation at 5 min intervals and 5000 rpm. Due to the heating in the centrifuge, samples were held in ice for 2 min after every 5 min filtration cycle. The centrifugation cycles were repeated until a total of 500 μ L of the filtered solution was collected. The stability over time of the filtered samples prepared according to this protocol was monitored by 1D spectra as shown in Figure S1 (right panels).

NMR Spectroscopy. All experiments were performed at 293 K using a Bruker Avance 700 NMR spectrometer. 2D saturation transfer difference and 1D-WG experiments were acquired with a 5 mm TCI CryoProbe, while 2D nonselective off-resonance relaxation experiments²⁴ were acquired with a TXI probe. For all experiments water suppression was achieved through a Watergate (WG) scheme implemented with the binomial 3-9-19 pulse train as explained before.²⁴ All 1D ¹H NMR spectra were recorded with 128 scans, 32 dummy scans, and spectral widths of 8389.26 Hz sampled with at least 4096 complex points. The repetition delay for all 1D experiments was 2 s. The peptide ¹H NMR signals were assigned using standard procedures.²⁵

2D Nonselective Off-Resonance Relaxation (ORR) Experiments.

Off-resonance relaxation data were acquired using the nonselective off-resonance relaxation 2D-TOCSY experiments.²⁴ The off-resonance spin lock with the trapezoidal shape was applied at an angle of 35.5° for 5, 23, 42, 60, and 80 ms with a strength of 8.23 kHz. For the TOCSY mixing, a 45 ms long 10 kHz DIPSI-2 pulse train was used. The interscan delay was 2 s, and for each sample two replicate experiments were acquired at each relaxation time. In each experiment, 8 scans and 128 dummy scans were employed. The spectral widths for both dimensions were 8389.26 Hz with 256 *t*₁ and 1024 *t*₂ complex points.

2D Saturation Transfer Difference (STD) Experiments.

The pulse sequence used for the 2D-STD NMR experiments²³ was implemented without the 30 ms spin-lock pulse to enhance the sensitivity, as the TOCSY spin-lock effectively serves already as an implicit relaxation filter. A train of 40 Gaussian-shaped pulses of 50 ms each separated by a 1 ms interpulse delay was applied to introduce selective saturation. The strength of each Gaussian pulse was 119 Hz with a 1% truncation and 1000 digitization points. The train of Gaussian pulses was preceded by a 100 ms delay in all STD experiments. The spectral widths for both dimensions were 8389.26 Hz and were digitized by 200 *t*₁ and 1024 *t*₂ complex points. The on-resonance irradiation was performed at the high-field pro-R γ V₁₈ methyl resonance (~0.7 ppm). As a result signals in the methyl region of the STD spectra do not reflect true STD effects but rather simply direct saturation by the selective RF. Our STD measurements therefore focused on the H α protons, which are not directly affected by the RF field of the Gaussian train used to introduce saturation. The off-resonance control irradiation was performed at 30 ppm. The saturation transfer difference (STD) spectrum

- (13) Klein, W. L.; Stine, W. B.; Teplow, D. B. *Neurobiol. Aging* **2004**, *25*, 569–580.
- (14) Kaye, R.; Head, E.; Thompson, J. L.; McIntire, M. T.; Milton, C.; Cotman, W. C.; Glabe, G. C. *Science* **2003**, *300*, 486–489.
- (15) Jarvet, J.; Damber, P.; Bodell, K.; Erkksson, L. E. G.; Graslund, A. *J. Am. Chem. Soc.* **2000**, *122*, 4261–4268.
- (16) Mansfield, L. S.; Jayawickrama, A. D.; Timmons, S. J.; Larive, K. C. *Biochim. Biophys. Acta* **1998**, *1382*, 257–265.
- (17) Zhang, S.; Casey, N.; Lee, P. J. *Folding Des.* **1998**, *3*, 413–422.
- (18) McLaurin, J.; Yang, D. S.; Yip, C. M.; Fraser, P. E. *J. Struct. Biol.* **2000**, *130*, 259–270.
- (19) Tycko, R. *Prog. Nucl. Magn. Reson. Spectrosc.* **2003**, *42*, 53–68.
- (20) Zagorski, M. G.; Yang, J.; Shao, H. Y.; Ma, K.; Zeng, H.; Hong, A. *Methods Enzymol.* **1999**, *309*, 189–204.
- (21) Ippel, J. H.; Olofsson, A.; Schleucher, J.; Lundgren, E.; Wijmenga, S. S. *Proc. Natl. Acad. Sci. U.S.A.* **2002**, *99*, 8648–8653.
- (22) Narayanan, S.; Bosl, B.; Walter, S.; Reif, B. *Proc. Natl. Acad. Sci. U.S.A.* **2001**, *100*, 9286–9291.
- (23) (a) Mayer, M.; Mayer, B. *J. Am. Chem. Soc.* **2001**, *123*, 6108–6117. (b) Mayer, M.; James, T. L. *J. Am. Chem. Soc.* **2002**, *124*, 13376–13377.
- (24) (a) Esposito, V.; Das, R.; Melacini, G. *J. Am. Chem. Soc.* **2005**, *127*, 9358–9359. (b) Milojevic, J.; Esposito, V.; Das, R.; Melacini, G. *J. Phys. Chem. B* **2006**, *110*, 20664–20670.

- (25) Wuthrich, K. *NMR of Proteins and Nucleic Acids*; John Wiley & Sons, Inc.: 1986.

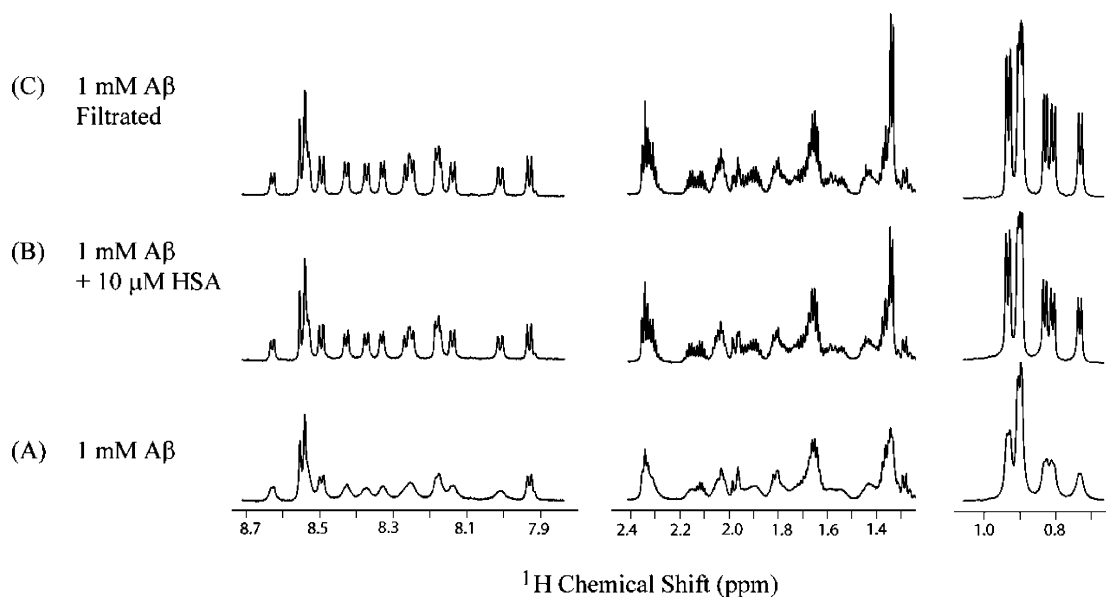


Figure 1. Effect of HSA addition and of 30 kDa cutoff filtration on the ^1H 1D-WG spectra of 1 mM $\text{A}\beta(12-28)$. (A) Unfiltered 1 mM $\text{A}\beta(12-28)$ before HSA addition. (B) Unfiltered sample after addition of 10 μM HSA. (C) 1 mM $\text{A}\beta(12-28)$ after 30 kDa filtration. All spectra were recorded at 700 MHz using a TCI CryoProbe and at 293 K with a 50 mM sodium acetate buffer- d_4 (pH 4.7). Different spectral regions are vertically scaled to optimally fit into the stacking space.

was obtained by phase cycling subtraction of the on-resonance and off-resonance data acquired in interleaved mode. The number of scans and dummy scans in the 2D-STD experiments were 16 and 128, respectively. Separate reference ST (STR) experiments were also acquired with 8 scans and 128 dummy scans.

Data Analysis. All 2D replicate data sets were added and processed using Xwinnmr (Bruker Inc.). Data were analyzed as previously published.^{23,24} Briefly, the 2D cross-peak intensities were measured using Sparky 3.111²⁶ by Gaussian line fitting and determination of fit heights.²⁴ The corresponding fit height error was estimated by calculating the standard deviation for the distribution of the differences in the intensities of identical peaks in duplicate spectra. After the addition of the duplicate spectra, the error was scaled up proportionally to the square root of the total number of scans. The TOCSY $\text{H}_{\alpha,i}-\text{H}_{\text{N},i}$ cross-peaks for residues [15–19], [21–24], and [26–28] were used for data analysis. For residues V_{12} , H_{14} , and F_{20} , the $\text{H}_{\alpha,12}-\text{H}_{\text{Me},12}$, $\text{H}_{\alpha,14}-\text{H}_{\beta\text{H},14}$, and $\text{H}_{\alpha,20}-\text{H}_{\beta\text{H},20}$ cross-peaks were used to avoid overlap and water exchange artifacts. G_{25} was omitted from the analysis of the off-resonance relaxation rates due to the degeneracy between its two H_{α} protons.²⁴ The nonselective off-resonance relaxation rates of decay were obtained through monoexponential fitting using the Curvefit program,²⁷ and errors in the fitted decay rates were obtained as previously explained.²⁴ The rates obtained through the nonlinear fitting, and the related errors were normalized with respect to the largest measured rate.

The saturation transfer ratios ($I_{\text{STD}}/I_{\text{STR}}$) were computed starting from the Sparky fit heights, correcting for the differences in the number of scans. The errors in the fit heights were evaluated as those for the nonselective off-resonance experiments and then were propagated to the ($I_{\text{STD}}/I_{\text{STR}}$) ratios. In the interpretation of these ratios, it should be considered that the saturation starts from the pro-R γ methyl of V_{18} and concurrently diffuses through both monomer- and oligomer-mediated pathways. While the contributions due to the oligomer-mediated spin diffusion usually prevail over those caused by the monomer-mediated pathways, the latter may not be fully negligible

for the directly saturated residue (i.e., V_{18}) and the adjacent amino acids.²²

Results and Discussion

The $\text{A}\beta(12-28)$ Peptide Includes Key Determinants of the $\text{A}\beta$ –HSA Interactions. As a first step toward the understanding of how human serum albumin (HSA) affects the prefibrillation oligomerization equilibria of $\text{A}\beta(12-28)$ we acquired 1D NMR spectra of this peptide in the absence and presence of HSA (Figure 1 A, B). The spectrum of 1 mM $\text{A}\beta(12-28)$ without HSA (Figure 1A) is line-broadened beyond the line width typically expected for single chain short 17-amino-acid peptides, indicating that monomeric $\text{A}\beta(12-28)$ is in a dynamic equilibrium with its prenuclear oligomers.^{15,16,28} Such oligomers are not an artifact of the peptide manufacturing process as previously shown¹⁵ and as also confirmed here in Figure S2 A–C and in Figure S3 A, B. These figures show that when oligomers are formed through different pathways, such as the addition of retentate or of salt to the filtered sample, a line-broadening similar to that observed for the unfiltered sample is obtained.

Upon addition of substoichiometric amounts ($\sim 1:100$) of HSA to the $\text{A}\beta(12-28)$ peptide, a dramatic line width reduction is observed (Figure 1B), similarly to the effect of filtration (Figure 1C). Analogous significant line-sharpening effects upon HSA addition are also observed when the oligomers are prepared through alternative methods (Figure S2 D and Figure S3 C). These observations are consistent with the hypothesis that HSA preferentially interacts with the line-broadening inducing $\text{A}\beta(12-28)$ oligomers rather than with the $\text{A}\beta(12-28)$ monomers, which would otherwise be line-broadened by HSA. In addition, the reduced line width occurring upon addition of HSA suggests also that the interaction of HSA with the $\text{A}\beta(12-28)$ oligomers interferes with the monomer–oligomer exchange, which causes the increased line widths observed in the absence of albumin (Figure 1A).^{15,28}

(26) Goddard, T. D.; Kneller, D. G. *Sparky 3.111*, SPARKY 3; University of California, San Francisco.

(27) Palmer, A. G. *Curvefit*; Department of Biochemistry and Molecular Biophysics, Columbia University: 630 West 168th Street, New York, NY 10032, 1998.

(28) Narayanan, S.; Reif, B. *Biochemistry* **2005**, *44*, 1444–1452.

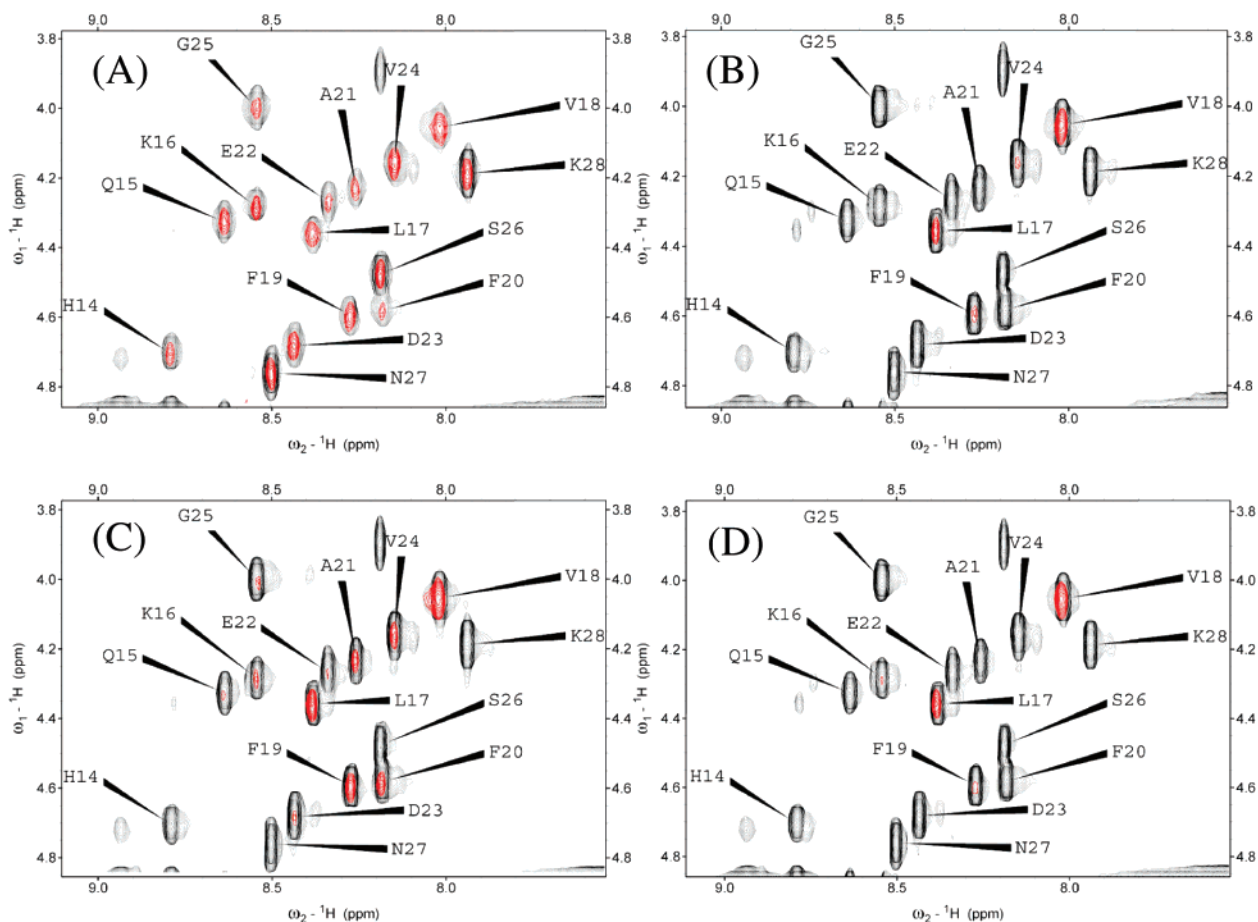


Figure 2. Effect of HSA addition and filtration on 2D saturation transfer difference and reference TOCSY spectra. In all panels the superimposition of the H_{α} – H_N fingerprint regions of the 2D-saturation transfer difference (red) and reference (black) spectra is shown. Panels (A) and (B) correspond to 1 mM A β (12–28) before and after 30 kDa cutoff filtration, respectively. Panels (C) and (D) refer to the unfiltered and filtrated 1 mM A β (12–28), respectively, both after addition of 10 μ M HSA. The lowest contour level for all spectra was set at 10 times the estimated noise. Spectra shown at lower contour levels are available in Figure S4. All spectra were measured at 700 MHz, 293 K in 50 mM sodium acetate buffer- d_4 (pH 4.7).

While these considerations clearly indicate that the A β (12–28) peptide under our experimental conditions includes key determinants for the A β –HSA interaction, the hypothesis on the preferential interaction of HSA with oligomeric rather than with monomeric A β (12–28) is somewhat counterintuitive. This is because the largely unstructured A β (12–28) peptide contains a central hydrophobic core (CHC) that drives its oligomerization,^{15–17,24} and HSA is known to bind hydrophobic ligands such as fatty acids. Therefore, before fully ruling out the interaction of HSA with the A β (12–28) monomers, we further investigated the HSA/A β (12–28) system using more advanced methods, such as 2D-saturation transfer difference^{22,23} and 2D-nonspecific off-resonance relaxation experiments,²⁴ which probe self-recognition with high sensitivity and resolution.

HSA Does Not Interact with the A β (12–28) Monomers.

Saturation transfer experiments have been used in the past to detect weak binding of small ligands to proteins with high sensitivity.²³ In addition, more recently STD experiments have been applied to amyloidogenic peptides proving that saturation transfer is very sensitive to oligomerization.^{22,28} We therefore acquired 2D-saturation transfer difference TOCSY experiments for the A β (12–28) peptide under several conditions with the purpose of investigating the effect of HSA on both monomers and oligomers. Figure 2 shows the H_N – H_{α} fingerprint regions of the saturation transfer difference TOCSY spectra (STD) (red

and the corresponding reference spectra (STR) (black) for a 1 mM A β (12–28) sample without and with HSA (panels A and C, respectively). In the absence of HSA an intense STD signal arising from the monomer–oligomer exchange is observed (Figure 2A). After addition of HSA the intensity of the STR cross-peaks increases due to the slower transverse relaxation but the intensity of the STD signal decreases relative to that of the STR spectrum (Figure 2C). This is also shown more quantitatively in Figure 3A where the normalized I_{STD}/I_{STR} ratios obtained for the H_N – H_{α} fingerprint regions are plotted vs the A β (12–28) sequence. Figure 3A clearly illustrates that the I_{STD}/I_{STR} ratios decrease after HSA addition for all residues in agreement with the line sharpening observed in the 1D spectra (Figure 1). These observations are consistent with the absence of interactions between HSA and the monomeric peptide as hypothesized above. However, an alternative and more trivial explanation is also possible; i.e., the small 1:100 substoichiometric amount of added HSA could be saturated by the A β (12–28) oligomers and therefore not be able to interact with the peptide monomers. In order to rule out this possibility, we acquired additional saturation transfer difference data. First, we performed STD experiments where HSA was added to a filtered sample, devoid of most line-broadening inducing oligomers. As a second control, we have also acquired STD spectra for 1 mM

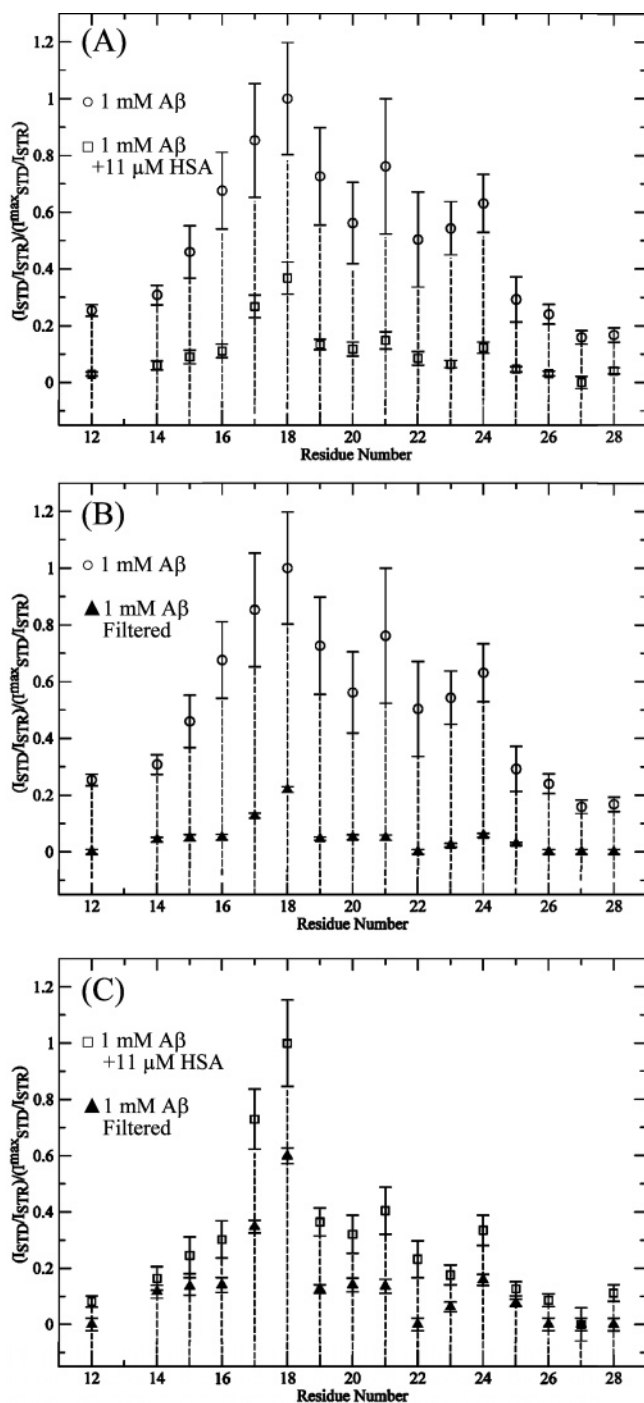


Figure 3. Effect of HSA addition and filtration on the saturation transfer H_{α} – H_N ratios. (A) Effect of HSA on the saturation transfer ratios of unfiltered 1 mM $A\beta(12-28)$. Circles and squares correspond to unfiltered 1 mM $A\beta(12-28)$ before and after 11 μM HSA addition, respectively. All ratios were normalized to the maximum saturation transfer ratio measured in the absence of HSA. (B) Effect of filtration on the saturation transfer ratios of 1 mM $A\beta(12-28)$. Circles and filled triangles correspond to 1 mM $A\beta(12-28)$ before and after filtration, respectively. All ratios were normalized to the maximum saturation transfer ratio measured before filtration. (C) Comparison of the effects of HSA and filtration. Full triangles and squares correspond to 1 mM $A\beta(12-28)$ after filtration and to unfiltered 1 mM $A\beta(12-28)$ after 11 μM HSA addition, respectively. All ratios were normalized to the highest ratio measured for 1 mM $A\beta(12-28)$ in the presence of the HSA. Each set of saturation transfer ratios appears twice in this figure in order to facilitate comparisons among different experimental conditions.

$A\beta(12-28)$ with increasing HSA concentrations (i.e., we performed an HSA titration).

For the control filtration STD experiments, a 1 mM $A\beta(12-28)$ sample was passed through a 30 kDa filter, and the resulting ST spectra and normalized I_{STD}/I_{STR} ratios are shown in Figures 2B and 3B, respectively. The comparison between panels 2A and 2B as well as Figure 3B clearly indicates that the 30 kDa filtration removed most of the oligomers generating the STD effect, with the residual STD signal observed for residues 17 and 18 likely being an artifact of the selected saturation frequency, as discussed in the Materials and Methods section. Therefore the filtered sample is devoid of the potentially HSA saturating peptide oligomers. Additionally, the absence of “seed” oligomers that may nucleate further oligomerization makes the filtered samples stable.^{15,29} The origin of such stability may be not only kinetic but also thermodynamic due to possible dilution effects occurring upon filtration. Upon addition of 10 μM HSA to the filtered sample no significant changes were detected by STD, as shown in Figure 2D and confirmed by Figures S4–S7. The similarity between the 2D-spectra shown in panels 2B and 2D strongly suggests that HSA does not interact with the $A\beta(12-28)$ monomers and possibly with residual unfiltered low MW oligomers, even after the potentially HSA-saturating oligomers have been removed by filtration. It should however be noticed that the interactions with oligomers characterized by MW < 10 kDa may possibly escape detection by the STD method.

The lack of $A\beta$ monomer–albumin interactions is also independently supported by our HSA titration study monitored by STD experiments (Figure 4). As expected, the titration plots reveal that the I_{STD}/I_{STR} ratios decrease as the HSA concentration is increased (Figure 4) until an asymptotic behavior is reached for all residues at HSA concentrations in the $\sim 8-10 \mu\text{M}$ range. Further addition of HSA above 8–10 μM does not significantly affect the I_{STD}/I_{STR} ratios, consistently with the absence of HSA–monomeric $A\beta(12-28)$ interactions. In summary, based on the above analysis we have conclusively demonstrated that HSA does not recognize the monomeric $A\beta(12-28)$ peptide. This result leads therefore to the still open question of defining which $A\beta(12-28)$ oligomerization states are able to recognize HSA.

HSA Recognition Competent States. In order to establish the molecular weight range for the oligomers that are able to interact with HSA, the results from the STD experiments in the presence of HSA were compared to the results obtained after 30 kDa cutoff filtration (Figures 2B, C and 3C). Both Figures 2C and 3C show that upon addition of HSA the I_{STD}/I_{STR} ratios decrease but not to the extent observed upon filtration (Figure 2B). This observation suggests that the addition of HSA does not completely prevent monomer–oligomer exchange. In other words the oligomers interacting with HSA are only a subset of those eliminated by filtration. When HSA interacts with $A\beta(12-28)$ oligomers with MWs larger than a critical value, the residues of monomeric $A\beta(12-28)$ become shielded from these oligomers, explaining the line sharpening (Figure 1) and the reduced I_{STD}/I_{STR} ratios observed upon HSA addition (Figure 3A).

(29) Bernstein, S. L.; Wyttenbach, T.; Baumketner, A.; Shea, J. E.; Bitan, G.; Teplow, D. B.; Bowers, M. T. *J. Am. Chem. Soc.* **2005**, *127*, 2075–2084.

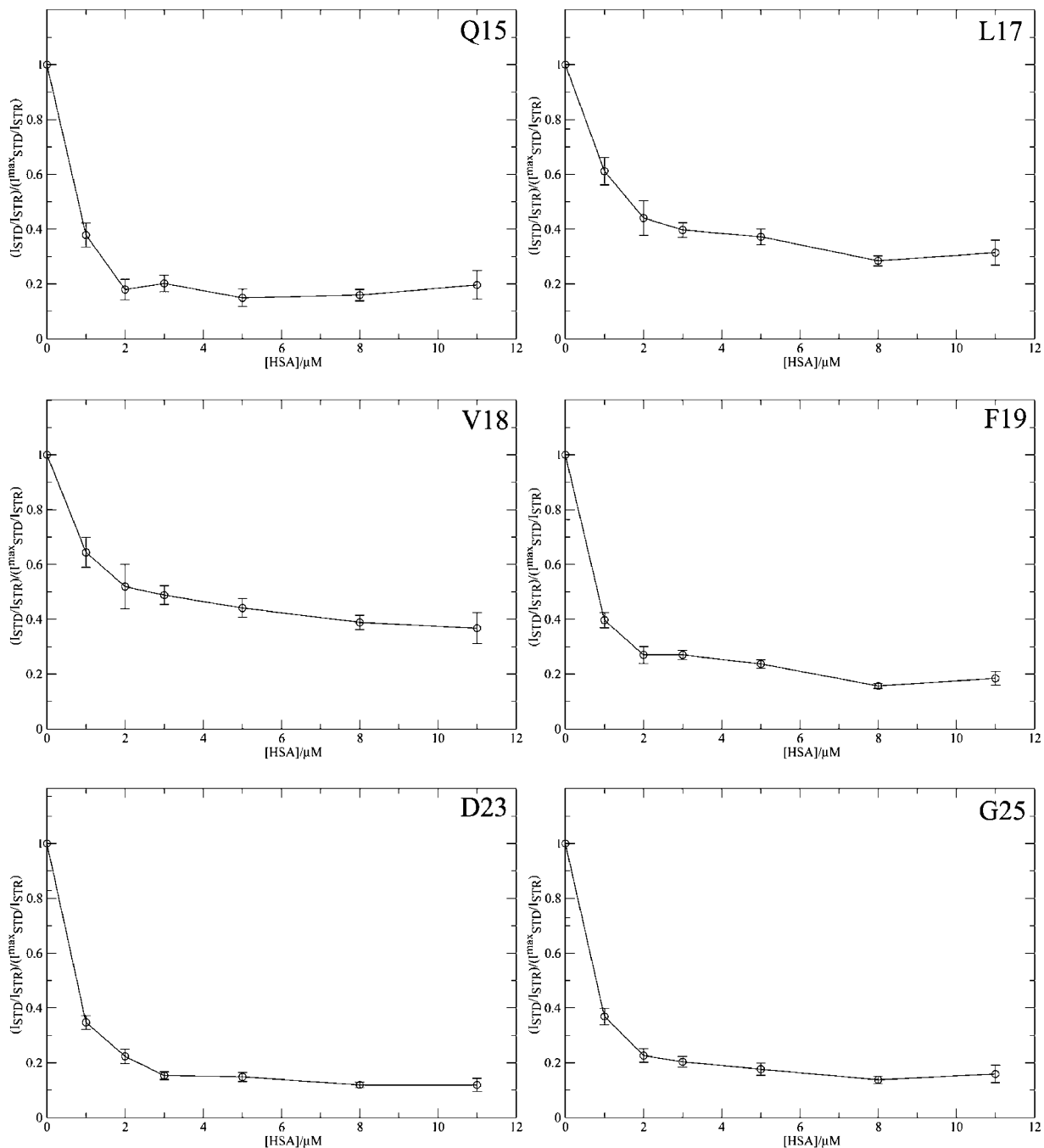


Figure 4. Saturation transfer titration curves for representative residues. Decreases in the I_{STD}/I_{STR} ratio of the H_{α} - H_N cross-peaks are observed as the HSA concentration increases until an asymptotic regime is reached. All ratios were normalized to their maximum value measured before adding HSA.

Accounting for the Observed Selectivity of Albumin for the High MW A β Oligomers. Our integrated NMR analysis conclusively reveals that under our experimental conditions HSA recognizes preferentially the high MW oligomers of A β (12–28), while no interactions were detected with the low MW assemblies or with the monomers. This result is quite intriguing because HSA is known to bind hydrophobic ligands, and therefore it is reasonable to think that HSA would target the highly hydrophobic core of the primarily unstructured monomeric A β (12–28) peptide.¹⁵ However, this scenario is clearly inconsistent with our experimental data. Furthermore, no binding could be detected by surface plasmon resonance between immobilized biotinylated A β (1–40) peptides and albumin,¹⁰ in

full agreement with our solution results on the lack of interactions between albumin and monomeric A β (12–28).

A possible explanation for this apparent paradox is that despite the fact that A β (12–28) is largely unstructured,¹⁵ residual local structure is still present in the monomeric peptide. For instance, small populations of structures with turnlike or helical conformational preferences have been proposed for A β peptides,³⁰ and the upfield shift at ~ 0.7 ppm of the pro-R methyl of V₁₈ observed for A β (12–28) has been accounted for in terms of intramolecular contacts between F₁₉F₂₀ and V₁₈.¹⁷ It is

(30) (a) Riek, R.; Guntert, P.; Dobeli, H.; Wipf, B.; Wuthrich, K. *Eur. J. Biochem.* **2001**, *268*, 5930–5936. (b) Zhang, S.; Iwata, K.; Lachenmann, M. J.; Peng, J. W.; Li, S.; Stimson, E. R.; Lu, Y.; Felix, A. M.; Maggio, J. E.; Lee, J. P. *J. Struct. Biol.* **2000**, *130*, 130–141.

therefore possible that these local interactions present in monomeric $A\beta$ prevent HSA from recognizing the single $A\beta$ -(12–28) peptide chains. It is also possible that the interaction of HSA with monomeric $A\beta$ (12–28) is entropically unfavorable. For instance, we can assume that monomers are significantly more flexible than oligomers, and therefore binding would cause large entropy losses making this process thermodynamically unfavorable. Oligomers, on the other hand, are expected to be more structured as a result of self-association, and therefore the entropy losses that occur upon binding are not as significant as those for the monomers.

In the low MW oligomers the HSA recognition motif may not yet be fully stabilized explaining why HSA is not able to bind small oligomers. Similar results were obtained with an antibody designed to target higher molecular weight oligomers. It was observed that the antibody did not crossreact with the low MW assemblies¹⁴ suggesting that there is a significant structural difference between lower and higher molecular weight oligomers. Finally, it should also be considered that another possible explanation for the selectivity of HSA toward the high MW oligomers is that the multiple polypeptide chains in each oligomer may provide additional recognition motifs absent in the monomers; i.e., oligomers might behave as a multivalent ligand, and this multivalency may be required for binding to HSA. The next question to address is whether the shielding of monomeric $A\beta$ (12–28) caused by HSA binding to the oligomers is selective for a specific subset of $A\beta$ (12–28) residues or it is a global effect involving all residues in $A\beta$ (12–28).

HSA Prevents All Residues of Monomeric $A\beta$ (12–28) from Interacting with Oligomeric $A\beta$ (12–28). A careful analysis of the STD and of the 1D spectra (Supporting Information, p S2) indicates that these experiments cannot provide reliable information about the shielding selectivity. These limitations can be overcome by using a recently published nonselective off-resonance relaxation experiment.²⁴ Specifically, Figures S8 and 5A show the observed nonselective off-resonance relaxation decays and the corresponding rates, respectively, before and after HSA addition. As expected, a significant decrease of H_{α} - $R_{35.5^{\circ}, ns}$ relaxation rates measured for the 1 mM $A\beta$ (12–28) sample is observed upon addition of 10 μ M HSA for most residues (Figure S8 and 5A). In addition, the changes in relaxation rates caused by HSA (Figure 5A) correlate well with those caused by filtration (Figure 5B, correlation coefficient of 0.96). Considering that filtration physically removes the oligomers from the solution without any residue specificity, the good correlation observed in Figure 5B suggests that, as a result of HSA addition, *all* residues of monomeric $A\beta$ (12–28) are equally shielded from the oligomers.

Toward a Model of $A\beta$ Oligomerization Inhibition by HSA. Another question that is still open is how albumin can recognize the hydrophobic patches of the oligomers since the oligomerization is driven by the shielding of the central hydrophobic core of the $A\beta$ (12–28) peptide^{16,17} and therefore the hydrophobic core of the oligomers is expected to be significantly more shielded relative to the monomers. A possible explanation is that HSA targets the $A\beta$ (12–28) oligomers at sites where new monomers bind during the growth of the peptide assembly (“growing loci”) and possibly also at sites transiently exposed to the solvent during the monomer/oligomer exchange

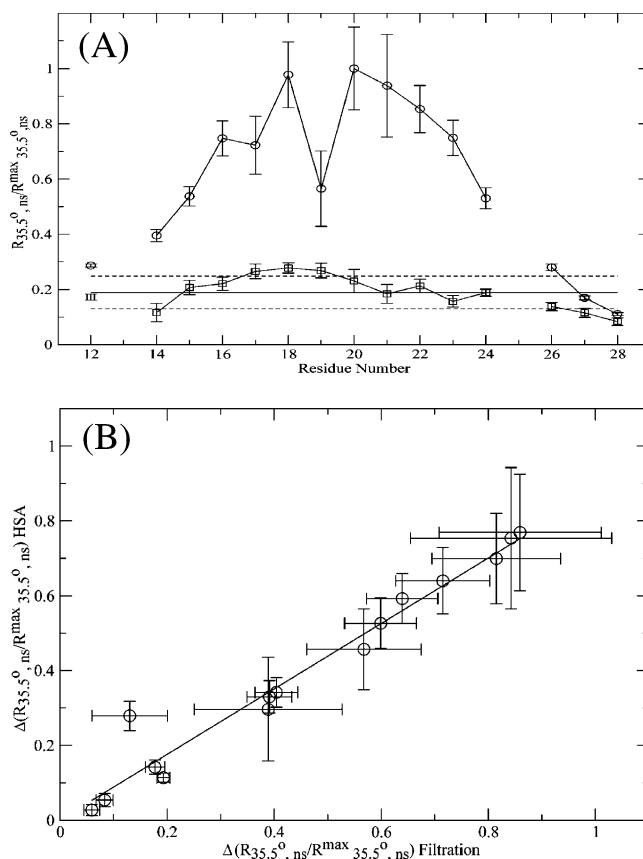


Figure 5. Effect of HSA on the nonselective off-resonance H_{α} relaxation rates. (A) Plot of relative $R_{35.5^{\circ}, ns}$ relaxation rates vs residue number in $A\beta$ (12–28). Circles correspond to 1 mM $A\beta$ (12–28) in the absence of HSA, while squares correspond to 1 mM $A\beta$ (12–28) in the presence of 10 μ M HSA. All rates were normalized to the maximum rate of the two sets ($R_{35.5^{\circ}, ns}^{max}$), as explained before.²⁴ All rates were measured at 293 K in 50 mM d_4 -sodium acetate buffer at pH 4.7 and 700 MHz. Solid and dashed lines indicate the mean \pm the standard deviation of the $R_{35.5^{\circ}, ns}$ rates measured for the sample containing 10 μ M HSA. (B) Linear correlation between the variations in $R_{35.5^{\circ}, ns}$ rates caused by filtration and by HSA addition. The horizontal axis refers to the difference between the normalized $R_{35.5^{\circ}, ns}$ relaxation rates measured for 1 mM $A\beta$ (12–28) before and after filtration, while the vertical axis refers to the difference between the normalized $R_{35.5^{\circ}, ns}$ relaxation rates measured for 1 mM $A\beta$ (12–28) in the absence and presence of 10 μ M HSA.

process (“exchange loci”). At these sites hydrophobic residues are available for HSA recognition. The binding of HSA to a range of soluble $A\beta$ (12–28) oligomers (Figure 6) would then block the further monomer addition and/or the monomer exchange with the peptide assemblies. This model accounts not only for the known oligomerization inhibitory function of HSA but also for the marked reductions in ORR rates and I_{STD}/I_{STR} ratios observed in our 2D experiments upon HSA addition (Figures 3 and 5). Furthermore, the shielding by HSA of the hydrophobic “growing or exchange loci” recognition motives can also explain why all residues of the monomer are equally blocked from the interaction with the oligomers.

Some general considerations can be drawn about the nature of the oligomer binding sites for HSA, i.e., the hypothesized “growing loci” and “exchange loci”, based on the possible symmetries of the oligomer overall morphology. Two main groups of $A\beta$ oligomeric assemblies have been proposed so far: oligomers with translational symmetry and oligomers with

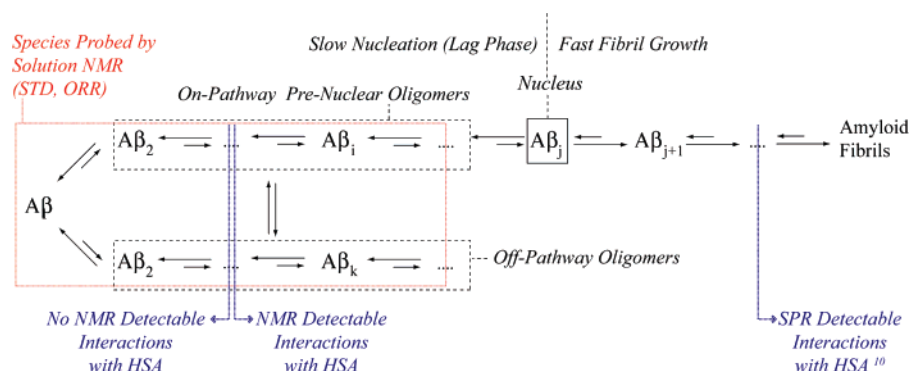


Figure 6. Proposed schematic model for the interactions between HSA and the oligomers of the A β peptide. The notation A β_n refers to an assembly of n polypeptide chains with the value of n increasing from left to right. Soluble off- and prenuclear on-pathway oligomers are denoted with black dashed boxes to differentiate them from other states involved in the general nucleation/growth mechanism.^{41,42} The red dotted box indicates the A β assemblies that are probed by solution NMR through saturation transfer difference (STD) and nonselective off-resonance relaxation (ORR) experiments. In blue we specify which species are human serum albumin (HSA)-binding competent. Further details about the nature of the interactions between HSA and the soluble oligomers are provided in the text. The NMR data presented here cannot differentiate between on- and off-pathway oligomers and are not relevant for the interactions with the postnuclear oligomers or with the fibrils. However, previous surface plasmon resonance (SPR) investigations did report binding interactions between A β fibrils and HSA.¹⁰

spherical symmetry.³¹ For the former class, including unit protofibrils and disc-shaped assemblies,³² growing or exchange loci can be envisaged at the tips of the oligomers similarly to what has been proposed for the fibrillar growth through monomer attachment at the end of existing fibrils, where exposed hydrophobic patches (e.g., residues 17–21) remain available.³³ For the latter class of oligomers with spherical symmetry,³⁴ including micellar aggregates,³¹ ADDLs (i.e., A β -derived diffusible ligands),³⁵ amylospheroids,³⁶ and β -amy balls,^{34,37} the identification of exposed hydrophobic stretches is less obvious. Nevertheless, it is possible that monomer addition to these oligomers occurs through a two-step “dock–lock” mechanism previously proposed for the A β deposition onto amyloid templates.³⁸ According to the “dock–lock” hypothesis, monomers in solution would first only loosely bind (“dock”) the pre-existing A β assemblies, and the incorporation into the core of the oligomer (“locking”) with full burial of the central hydrophobic core of A β would occur only later, when the subsequent A β monomer docks. Therefore, if albumin recognizes partly exposed hydrophobic residues at the docking site of the oligomer, further growth of the A β assembly would be halted according to the “dock–lock” mechanism.

One possible alternative model for the inhibition by HSA of the A β monomer–oligomer association might also be the disruption of A β oligomers by albumin. A possible mechanism

for such oligomer disruption is through their destabilization relative to the monomers, i.e., through monomer stabilization. However, we did not observe any interaction between HSA and the monomers, which could potentially account for such monomer stabilization. On the contrary, we did observe a preferential interaction of HSA with the oligomers. Therefore, while oligomer disruption cannot be fully ruled out at the present stage, it is possible that the oligomers are still present in solution. In addition, the decay/plateau trend observed for the STD-monitored titration plots (Figure 4) is fully consistent with HSA binding to the existing oligomers, causing the decay, until all binding sites in the oligomers are saturated with HSA, causing the plateau. Furthermore, other proteins with fibrillogenesis inhibitory functions such as apolipoprotein E3 (ApoE3) and heat shock protein 70 (Hsp70) have been shown to target and bind prefibrillar oligomers, as discussed below.^{39,40}

Comparison with Other A β Oligomerization Inhibitory Systems. The model proposed here for the inhibitory function of HSA with respect to A β oligomerization (Figure 6) may also apply to other systems. For instance, the apolipoprotein E3 represents another endogenous inhibitor of amyloid formation, and it is known that ApoE3 specifically targets prenuclear oligomers, thus interfering with the nucleation process required for fibril formation.³⁹ Furthermore, it has been recently found⁴⁰ that the fibrillization of α -synuclein is inhibited by the chaperone Hsp70 using a mechanism in which Hsp70 selectively recognizes prefibrillar oligomeric rather than monomeric α -synuclein. Upon binding the α -synuclein oligomers, this chaperone caps available hydrophobic patches thus inhibiting the progression of α -synuclein assemblies toward amyloid fibrils.

The similarity between the oligomerization inhibitory mechanism proposed for the HSA/A β system and those reported for other systems suggests that the model put forward for HSA (Figure 6) may represent a more general paradigm defining a shared cellular defense strategy against amyloid-related diseases. This conclusion is supported by the recent discovery that different amyloidogenic protein sequences lead to prefibrillar

(31) Tiana, G.; Simona, F.; Broglia, R. A.; Colombo, G. *J. Chem. Phys.* **2004**, *120*, 8307–8317.

(32) Mastrangelo, I. A.; Ahmed, M.; Sato, T.; Liu, W.; Wang, C.; Hough, P.; Smith, S. O. *J. Mol. Biol.* **2006**, *358*, 106–119.

(33) Luhrs, T.; Ritter, C.; Adrian, M.; Riek-Loher, D.; Bohrmann, B.; Döbeli, H.; Schubert, D.; Riek, R. *Proc. Natl. Acad. Sci. U.S.A.* **2005**, *102*, 17342–17347.

(34) Chimon, S.; Ishii, Y. *J. Am. Chem. Soc.* **2005**, *127*, 13472–13473.

(35) Chromy, B. A.; Nowak, R. J.; Lambert, M. P.; Viola, K. L.; Chang, L.; Velasco, P. T.; Jones, B. W.; Fernandez, S. J.; Lacor, P. Horowitz, P.; Finch, C. E.; Krafft, G. A.; Klein, W. L. *Biochemistry* **2003**, *42*, 12749–12760.

(36) Hoshi, M.; Sato, M.; Matsumoto, S.; Noguchi, A.; Yasutake, K.; Yoshida, N.; Sato, K. *Proc. Natl. Acad. Sci. U.S.A.* **2003**, *100*, 6370–6375.

(37) Westlind-Danielsson, A.; Arnerup, G. *Biochemistry* **2001**, *40*, 14736–14743.

(38) Esler, W. P.; Stimson, E. R.; Jennings, J. M.; Vinters, H. V.; Ghilardi, J. R.; Lee, J. P.; Mantyh, P. W.; Maggio, J. E. *Biochemistry* **2000**, *39*, 6288–6295.

(39) Evans, K. C.; Berger, E. P.; Cho, C. G.; Weisgraber, K. H.; Lansbury, P. T. *Proc. Natl. Acad. Sci. U.S.A.* **1995**, *92*, 763–767.

(40) Dedmon, M.; Christodoulou, J.; Wilson, R. M.; Dobson, M. C. *J. Biol. Chem.* **2005**, *280*, 14733–14740.

(41) Come, J. H.; Fraser, P. E.; Lansbury, P. T. *Proc. Natl. Acad. Sci. U.S.A.* **1993**, *90*, 5959–5963.

(42) Jarrett, J. T.; Lansbury, P. T. *Cell* **1993**, *73*, 1055–1058.

soluble oligomers with a common structure and a common pathogenic mechanism^{14,40} despite their sequence variability.

Pharmacological Relevance. The model of Figure 6 is also pharmacologically relevant. First, the hydrophobic capping mechanism may be used as a general therapeutic strategy to trap the early soluble oligomers and block further oligomerization. Second, considering that under physiological conditions plasma $A\beta$ is mainly bound to HSA, it is clear that the HSA– $A\beta$ interactions may play a central role in the pathology of AD. The presence of these interactions has therefore to be taken into account when designing drug therapies. For instance, the administration of drugs competing with the $A\beta$ oligomers for the same HSA binding sites, as was previously reported for the antidiabetic medication tolbutamide,¹⁰ can cause the displacement of the $A\beta$ oligomers from albumin thus enhancing β -amyloid formation and therefore possibly promoting the development of AD. This means that the effective target for amyloid treatments is not simply the $A\beta$ peptide but the complex system composed of both albumin and the $A\beta$ peptide.

Conclusions

The comparative NMR analysis of 1D and 2D STD and ORR experiments of filtered and inhibited states of $A\beta(12-28)$ has revealed that HSA inhibits $A\beta$ oligomerization by selectively recognizing a distribution of soluble high MW prefibrillar

oligomers and targeting their exposed hydrophobic loci. As a result of albumin capping these hydrophobic patches, the addition of further monomers is blocked and the growth of the oligomers is inhibited. This oligomerization inhibition strategy may represent a general cellular defense scheme, and it may also open new perspectives in the design of anti-amyloid therapies. Furthermore, the filtration based ORR/STD NMR approach employed here to investigate the inhibitory mechanism of albumin is generally applicable to other oligomerization inhibitors as well as to other amyloidogenic systems.

Acknowledgment. We thank NSERC, the Alzheimer Society of Canada, and the Canadian Institutes of Health Research (CIHR) for financial support to G.M. G.M. is also grateful to the Heart and Stroke Foundation of Canada for a Maureen Andrew New Investigator award, and V.E., to the Federico II University of Naples for a graduate fellowship. We thank Hao Huang, Leslie Reid, and Karin A. Stephenson for helpful discussions.

Supporting Information Available: Further details on the analysis of the STD and 1D spectra, on ref 4, and on further control experiments. This material is available free of charge via the Internet at <http://pubs.acs.org>.

JA067367+